AMERICAN SOCIETY FOR MICROBIOLOGY | Applied and Environmental Microbiology

A 2-Hydroxypyridine Catabolism Pathway in *Rhodococcus rhodochrous* Strain PY11

Justas Vaitekūnas, Renata Gasparavičiūtė, Rasa Rutkienė, Daiva Tauraitė, Rolandas Meškys

Department of Molecular Microbiology and Biotechnology, Institute of Biochemistry, Vilnius University, Vilnius, Lithuania

Rhodococcus rhodochrous **PY11 (DSM 101666) is able to use 2-hydroxypyridine as a sole source of carbon and energy. By investigating a gene cluster (*hpo*) from this bacterium, we were able to reconstruct the catabolic pathway of 2-hydroxypyridine degradation. Here, we report that in *Rhodococcus rhodochrous* PY11, the initial hydroxylation of 2-hydroxypyridine is catalyzed by a four-component dioxygenase (HpoBCDF). A product of the dioxygenase reaction (3,6-dihydroxy-1,2,3,6-tetrahydropyridin-2-one) is further oxidized by HpoE to 2,3,6-trihydroxypyridine, which spontaneously forms a blue pigment. In addition, we show that the subsequent 2,3,6-trihydroxypyridine ring opening is catalyzed by the hypothetical cyclase HpoH. The final products of 2-hydroxypyridine degradation in *Rhodococcus rhodochrous* PY11 are ammonium ion and α-ketoglutarate.**

Pyridine and its derivatives are ubiquitous in nature. The pyridine ring is found in alkaloids (e.g., nicotine, actinidine), coenzymes [NAD(P)H, pyridoxal], and man-made solvents, pesticides, and herbicides (e.g., paraquat). Hydroxypyridines are common intermediate metabolites produced during microbial biodegradation of various *N*-heterocycles (pyridine, nicotine, picoline, 2,6-dipicolinic acid) (1–3).

It has previously been reported that *Arthrobacter crystallopoietes*, *Arthrobacter pyridinolis*, and *Arthrobacter viridescens* (4), *Achromobacter* sp. strain G2 (5), and *Nocardia* sp. strain PNO (6) use 2-hydroxypyridine (2HP) as a sole carbon and energy source. Through more than 50 years of investigation of pyridine ring metabolism, many intermediates have been identified and metabolic pathways have been proposed. However, the genes and enzymes responsible for 2HP biodegradation have seldom been reported.

In *Achromobacter* sp. G2, 2HP is metabolized via the maleamate pathway (5) (Fig. 1). No enzymes responsible for the initial hydroxylation step of 2HP leading to the formation of 2,5-dihydroxypyridine (2,5DHP) have been reported to date. Nevertheless, the degradation of 2,5DHP, an intermediate of nicotinic acid metabolism, has been fully investigated by Jiménez et al. (7), and all genes encoding the enzymes involved in the maleamate pathway have been identified and characterized (7).

Arthrobacter crystallopoietes, *A. pyridinolis*, and *A. viridescens* (4) and *Arthrobacter* sp. strain PY22 (8) produce a blue pigment (nicotine blue) in the medium when grown on 2HP. The nicotine blue has been shown to be a 4,5,4′,5′-tetrahydroxy-3,3′-diazadiphenoquinone-(2,2′) (9) that is an autoxidation product of 2,3,6-trihydroxypyridine (THP). THP can be synthesized via hydroxylation of 2,5DHP, 2,3-dihydroxypyridine (2,3DHP), or 2,6-dihydroxypyridine (2,6DHP); however, only the 2,6DHP 3-hydroxylase, which is involved in the biodegradation of nicotine by *Arthrobacter nicotinovorans*, has been identified to date (10).

We have previously reported that HpyB monooxygenase from *Arthrobacter* sp. PY22 is sufficient for the conversion of 2HP to THP (8). Since no reaction intermediates have been detected, a consecutive two-step hydroxylation of the substrate has been proposed. Further steps of this pathway, which has not been fully elucidated yet, most probably include maleamic acid (6) or α-ketoglutarate (11, 12).

Various hydroxypyridines (e.g., 3-hydroxypyridine, 2,3DHP, and 2,6DHP) have been identified to be intermediates in the degradation of pyridine compounds by *Arthrobacter crystallopoietes* and *Rhodococcus opacus* (Fig. 1). While the detailed analysis of intermediate metabolites has allowed the steps leading to pyridine biodegradation in the aforementioned bacteria to be described, no enzymes involved in this bioconversion have been identified yet (13).

In this study, we report the characterization of the 2HP catabolic pathway in *Rhodococcus rhodochrous* PY11, which has been isolated on the basis of its ability to utilize 2HP as a carbon source for growth (14). A gene cluster (*hpo*) encoding the proteins required for 2HP biodegradation in this bacterium has been identified and characterized. The intermediate metabolites have also been determined. We demonstrate that multicomponent HpoBCDF dioxygenase is responsible for the initial step of 2HP biodegradation. We also describe an enzymatic reaction of the ring opening of THP that is catalyzed by the hypothetical cyclase HpoH.

MATERIALS AND METHODS

Bacterial strains and growth conditions, plasmids, primers, and standard techniques. The 2HP-degrading bacterium *Rhodococcus rhodochrous* PY11 was previously isolated from a soil sample (14). The *Rhodococcus erythropolis* SQ1 strain (15) was chosen as the host strain for the expression of recombinant genes (cloned into plasmid pART2 [16] or pNitQC1 [17]) in bioconversion experiments. *Escherichia coli* strain DH5α was used for cloning experiments. The recombinant proteins were overexpressed in *E. coli* strain BL21(DE3). The bacterial strains, plasmids, and primers used in this study are listed in Table 1. *Rhodococcus* strains were grown at 30°C with aeration, and *E. coli* strains were grown at 37°C with aeration. *Rhodococcus rhodochrous* PY11 was cultivated either in nu-

Received 11 September 2015 **Accepted** 4 December 2015

Accepted manuscript posted online 11 December 2015

Citation Vaitekūnas J, Gasparavičiūtė R, Rutkienė R, Tauraitė D, Meškys R. 2016. A 2-hydroxypyridine catabolism pathway in *Rhodococcus rhodochrous* strain PY11. Appl Environ Microbiol 82:1264–1273. doi:10.1128/AEM.02975-15.

Editor: M. J. Pettinari, University of Buenos Aires

Address correspondence to Justas Vaitekūnas, justas.vaitekunas@bchi.vu.lt.

Supplemental material for this article may be found at http://dx.doi.org/10.1128/AEM.02975-15.

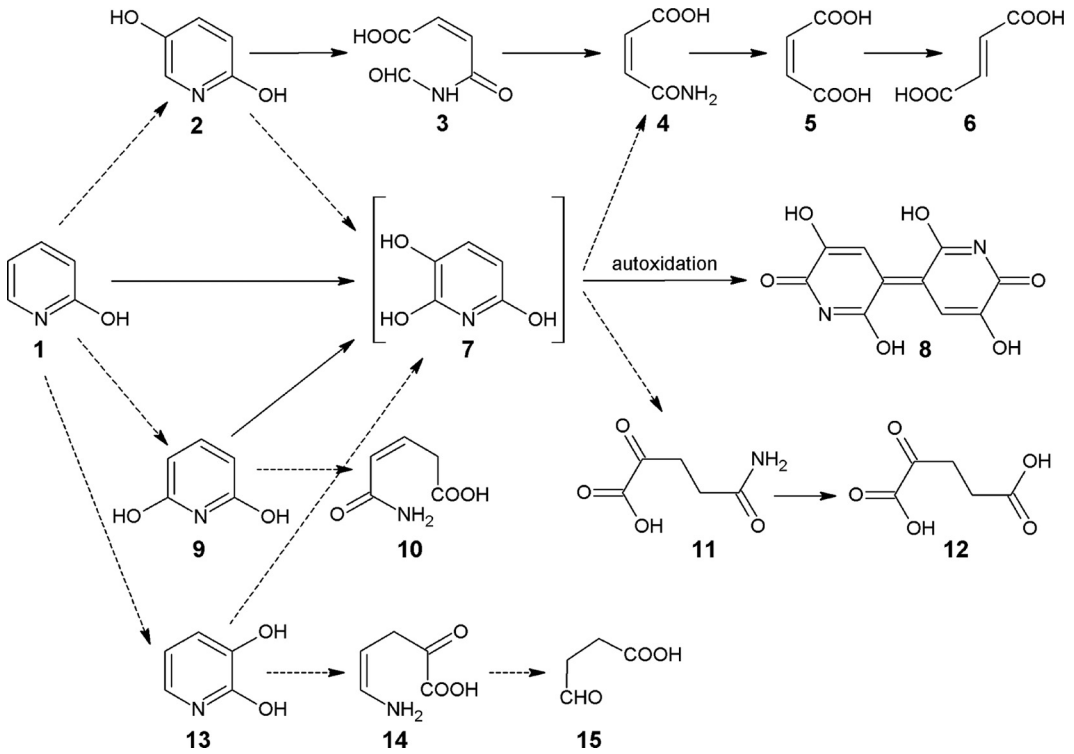

FIG 1 Proposed pathways of aerobic 2HP degradation in bacteria. Solid arrows, reactions for which the appropriate genes and/or enzymes are known; dashed arrows, proposed reactions. Compound 1, 2-hydroxypyridine; compound 2, 2,5-dihydroxypyridine; compound 3, *N*-formylmaleamic acid; compound 4, maleamic acid; compound 5, maleic acid; compound 6, fumaric acid; compound 7, 2,3,6-trihydroxypyridine; compound 8, nicotine blue pigment; compound 9, 2,6-dihydroxypyridine; compound 10, 3-pentenoic acid monoamide; compound 11, 2-ketoglutaramate; compound 12, α-ketoglutarate; compound 13, 2,3-dihydroxypyridine; compound 14, 5-amino-2-oxo-4-pentenoic acid; compound 15, succinic semialdehyde.

trient broth (NB) medium (Oxoid) or in minimal medium (5 g/liter NaCl, 1 g/liter K_2HPO_4, 1 g/liter $NH_4H_2PO_4$, 0.1 g/liter $MgSO_4$, 0.2 g/liter yeast extract, pH 7.2) supplemented with either 2HP (0.1% [wt/vol]) or succinate (0.1% [wt/vol]). *E. coli* cells transformed with recombinant plasmids were cultivated in NB medium supplemented with appropriate antibiotics (50 μg/ml ampicillin, 20 μg/ml streptomycin, or 40 μg/ml kanamycin). *R. erythropolis* SQ1 cells transformed with recombinant plasmids were grown in the presence of 60 μg/ml kanamycin or 30 μg/ml chloramphenicol. For transformation of plasmid DNA, electroporation was applied. Standard molecular biology techniques were performed as described previously (18).

mRNA differential display. Isolation of RNA from *Rhodococcus rhodochrous* PY11 was performed according to a previously published method (19). Reverse transcription (RT)-PCRs were performed as described in reference 20 with modifications. Five random primers were used for RT-PCR (Table 1). Arbitrarily amplified DNA fragments were generated from the total RNA of induced cells (0.1% 2HP) and control cells (0.1% succinate). A series of five parallel RT and PCR amplification reactions was performed using a cMaster RTplusPCR system (Eppendorf, Germany). The following temperature regime was applied: 94°C (5 min), 40°C (5 min), and 72°C (5 min) for 1 cycle, followed by 40 cycles of 94°C (1 min), 60°C (1 min), and 72°C (5 min). The DNA fragments were separated by electrophoresis in 8% polyacrylamide gels (18) and visualized by ethidium bromide staining. Bands generated from the RNA of induced cells but not from the RNA of control cells were excised from the gel and placed in a tube with distilled water. After 1 h of incubation, the water was discarded. In total, 50 μl of 10 mM Tris-HCl, pH 8.3, buffer containing 10 mM KCl was added, and the mixture was heated to 95°C for 1 h to allow some of the DNA to diffuse out of the gel. To reamplify the eluted DNA, the extracts were cleared by centrifugation and the supernatant was used as a template for the PCR. The reamplification conditions were as follows: 94°C (1 min), 60°C (1 min), and 72°C (5 min) for 40 cycles. Then, each DNA fragment was cloned into the pTZ57R/T vector and sequenced using M13/pUC (−46) forward 22-mer and reverse 24-mer primers.

Analysis of the protein expression profile induced by 2HP and purification of the 2HP-inducible protein from *Rhodococcus rhodochrous* PY11. *Rhodococcus rhodochrous* PY11 cells were grown in the presence of 2HP or succinate (control) in the minimal medium for 15 h, and then the cells were harvested, washed with 0.9% NaCl, resuspended in 50 mM Tris-HCl buffer, pH 8.0, and disrupted by sonication at 750 W for 15 min using a VC750 ultrasound processor (Sonics & Materials, Inc.). Cell debris was removed by centrifugation at 16,000 × *g* for 45 min. The resulting cell extract was used for SDS-PAGE analysis.

To purify the inducible 45-kDa protein, 1-liter flasks containing 200 ml of minimal medium supplemented with 2HP were inoculated with the overnight culture of *Rhodococcus rhodochrous* PY11 and incubated for 15 h under anaerobic conditions. Then, the cells were collected by centrifugation (4,000 × *g* for 20 min) and washed with 0.9% NaCl. Cell extracts were prepared by resuspending the cell paste in 50 mM Tris-HCl buffer, pH 7.5, containing 1 mM EDTA and 10% glycerol (buffer A). The cells were then disrupted by sonication, and the cell debris was removed by centrifugation (16,000 × *g* for 45 min). The cell extract was loaded onto a DEAE-Sepharose column (22 ml) that had been preequilibrated with buffer A. The column was then washed with buffer A, and the 45-kDa protein was eluted with a linear gradient from 0 to 1 M NaCl in buffer A. The fractions were checked by electrophoresis, and those containing the highest concentration of the 45-kDa protein were pooled, saturated with solid ammonium sulfate, and applied onto a phenyl-Sepharose column (20 ml) equilibrated with 25 mM Tris-HCl buffer, pH 7.5, containing 1.5 M am-

TABLE 1 Bacterial strains, plasmids, and primers used in this study

Strain, plasmid, or primer	Genotype or relevant characteristics, relevant properties and cloning strategies, or sequence (5′–3′)[a]	Reference or source
Strains		
Rhodococcus rhodochrous PY11	2HP-degrading bacterium	14
R. erythropolis SQ1	Mutant of *Rhodococcus erythropolis* strain ATCC 4277-1 with increased transformability	15
E. coli BL21(DE3)	F^- *ompT* $hsdS_B(r_B^-\ m_B^-)$ *gal dcm* (DE3), strain for protein overexpression	Novagen, Germany
E. coli DH5α	F^- ϕ80d*lacZ*ΔM15 Δ(*lacZYA-argF*)*U169 recA1 endA1 hsdR17*$(r_K^-\ m_K^+)$ *phoA supE44* λ^- *thi-1 gyrA96 relA1*	Fermentas, Lithuania
Plasmids		
pUC19	Ap^r *ori* ColE1 *lacZ*α, high copy-no. cloning vector	18
pTZ57R/T	Ap^r *ori* ColE1 *lacZ*α, high copy-no. cloning vector	Thermo Fisher Scientific, Lithuania
pET-21b	pBR322-derived ColE1, T7 *lac* promoter, Ap^r	Novagen, Germany
pET-28b	pBR322-derived ColE1, T7 *lac* promoter, Km^r	Novagen, Germany
pETDuet-1	pBR322-derived ColE1, T7 *lac* promoter, two MCSs,[a] Ap^r	Novagen, Germany
pCDFDuet-1	CloDF13 replicon, T7 *lac* promoter, two MCSs, Sm^r	Novagen, Germany
pART2	*E. coli-A. nicotinovorans* shuttle plasmid for *hdnOp*-driven constitutive expression, MCS, Km^r	16
pNitQC1	*E. coli-Rhodococcus* shuttle vector for constitutive expression, Chl^r *repAB*	17
pETDuet-hpoB	The *hpoB* gene was amplified by PCR using plasmid pHpoBCDEFG and primers hpoBF and hpoBR, digested with NdeI and XhoI, and cloned into the corresponding sites of the pETDuet-1 vector	This study
pCDFDuet-hpoC	The *hpoC* gene was amplified by PCR using plasmid pHpoBCDEFG and primers hpoCF and hpoCR, digested with NcoI and HindIII, and cloned into the pCDFDuet-1 vector cut with NcoI and HindIII	This study
pET21-hpoD	The *hpoD* gene was amplified by PCR using plasmid pHpoBCDEFG and primers hpoDF2 and hpoDR, digested with NdeI and HindIII, and cloned into the corresponding sites of the pET21b vector	This study
pCDFDuet-hpoF	The *hpoF* gene was amplified by PCR using plasmid pHpoBCDEFG and primers hpoFF and hpoFR, digested with BglII and KpnI, and cloned into the corresponding sites of the pCDFDuet-1 vector	This study
pB/D	The *hpoD* gene was amplified by PCR using plasmid pHpoBCDEFG and primers hpoDF1 and hpoDR, digested with EcoRI and HindIII, and cloned into the corresponding sites of the pETDuet-hpoB plasmid	This study
pF/C	The *hpoC* gene was amplified by PCR using plasmid pHpoBCDEFG and primers hpoCF and hpoCR, digested with NcoI and HindIII, and cloned into the corresponding sites of the pCDFDuet-hpoF plasmid	This study
pET28-hpoI	The *hpoI* gene was amplified by PCR using genomic DNA of *Rhodococcus rhodochrous* PY11 and primers hpoIF and hpoIR, digested with NdeI and XhoI, and cloned into the corresponding sites of the pET28b vector	This study
pART2HpoE	The *hpoE* gene was amplified by PCR using plasmid pHpoBCDEFG and primers hpoEF and hpoER, digested with KpnI and XbaI, and cloned into the corresponding sites of the pART2 vector	This study
pNitHpoBCD	The *hpoBCD* genes were amplified by PCR using plasmid pHpoBCDEFG and primers hpoBF and hpoDR, digested with NdeI and HindIII, and cloned into the corresponding sites of the pNitQC1 vector	This study
pHpoBCDEFG	A 5.2-kb Bsp1407I genomic DNA fragment containing the *hpoB*, *hpoC*, *hpoD*, *hpoE*, *hpoF*, and *hpoG* genes from *Rhodococcus rhodochrous* PY11 was inserted into the pART2 vector cut with Acc65I	This study
pNitHpoH	The *hpoH* gene was amplified by PCR using genomic DNA of *Rhodococcus rhodochrous* PY11 and primers hpoHF and hpoHR, digested with NcoI and HindIII, and cloned into the corresponding sites of the pNitQC1 vector	This study
Primers		
hpoBF	GCACATATGAGCACATACGTCTGCAAC	This study
hpoBR	CAGCTCGAGCTATGGCTGCGTGTTG	This study
hpoCF	CTACCATGGTGACCGCCACAGTGGATC	This study
hpoCR	CTAAAGCTTGGCATTGTTGGCTCGATTC	This study
hpoDF1	CTAGAATTCGATGCCTAAGCAGCTG	This study
hpoDF2	GCACATATGCCTAAGCAGCTGC	This study
hpoDR	CAGAAGCTTTCAGACATGAGCGGGA	This study
hpoFF	GACAGATCTCATGAGCACGATCGATG	This study

(Continued on following page)

TABLE 1 (Continued)

Strain, plasmid, or primer	Genotype or relevant characteristics, relevant properties and cloning strategies, or sequence (5′–3′)[a]	Reference or source
hpoFR	GACGGTACCTCAGATGTCGAGGATCAG	This study
hpoIF	CCTAGATCTCCATATGAGTAACCGGCTCG	This study
hpoIR	CATCTCGAGTCAGGCGACGCCGATCG	This study
hpoEF	CTCGGTACCCATGTCTGACGGCAAGGTC	This study
hpoER	GAGTCTAGATGTCACGAAGCCTCCGTC	This study
hpoHF	GTACCATGGGAACGGACCTGATCACCTC	This study
hpoFR	GATAAGCTTCCGATCACCGGTCCTCAG	This study
Primers for mRNA differential display		
RAN1	CGGAGCAGAAGACATGA	This study
RAN2	CGGAGCAGAAGACATGC	This study
RAN3	CGGAGCAGAAGACATGG	This study
RAN4	CGGAGCAGAAGACATGT	This study
RAN5	CGGAGCAGAAGACAATG	This study

[a] MCSs, multiple-cloning sites.

monium sulfate, 1 mM EDTA, and 10% (vol/vol) glycerol. The 45-kDa protein was eluted with a linear gradient of 1.5 to 0 M $(NH_4)_2SO_4$. After electrophoresis, the fractions of interest were pooled, concentrated with ammonium sulfate, and loaded onto a Superdex 200 column equilibrated with buffer A supplemented with 0.1 M NaCl. After gel filtration chromatography, the fractions were further purified by rechromatography on a Mono Q column (1 ml) equilibrated with buffer A. Fractions containing the 45-kDa protein were eluted with a linear gradient of 0 to 1 M NaCl in buffer A. The N-terminal sequence of the purified protein was determined by Edman degradation (Umea University, Umea, Sweden).

Cell suspension experiments and bioconversions. *R. erythropolis* SQ1 or *E. coli* cells transformed with recombinant plasmids carrying different genes of the *hpo* locus were cultivated as described above. For cell suspension and bioconversion experiments, *R. erythropolis* SQ1 was grown in 2-liter flasks containing 250 ml of NB medium until the culture reached an optical density at 600 nm (OD_{600}) of 1.6 to 2.0. *E. coli* BL21(DE3) cells were cultured aerobically at 30°C in 2-liter conical flasks with 250 ml of brain heart infusion (BHI) medium (Oxoid) supplemented with the appropriate antibiotics. When an OD_{600} of 1.2 was reached, 0.5 mM isopropyl-β-D-thiogalactopyranoside (IPTG) was added to induce the expression of proteins, and the culture was incubated for 20 h at 20°C. Then, cells were collected by centrifugation, washed twice, and resuspended in 10 mM potassium phosphate, pH 7.2, to achieve a 4-fold increase in cell density. The cell suspension was then supplemented with 0.1 to 0.2 mM appropriate substrate and incubated at 30°C. Bacteria were removed by centrifugation at 16,000 × *g* for 1 min, and the UV absorption spectrum of each supernatant was recorded in a PowerWave XS plate reader (BioTek Instruments, Inc.). Bioconversion reactions were carried out in a total volume of 250 ml at 30°C with shaking at 180 rpm. Substrate and glucose were added to the reaction mixture in portions of 20 mg and 125 mg, respectively, while the progress of conversion was monitored by determination of the changes in the UV absorption spectrum in the 200- to 340-nm range.

Metabolite detection, isolation, and structural analysis. High-performance liquid chromatography (HPLC)-mass spectrometry (MS) analyses were performed using a high-performance liquid chromatography system (Shimadzu, Japan) equipped with a photodiode array (PDA) detector (Shimadzu, Japan) and mass spectrometer (LCMS-2020; Shimadzu, Japan) equipped with an electrospray ionization source. The chromatographic separation was conducted using a Hydrosphere C_{18} column (4 mm by 150 mm; YMC, Japan) at 40°C and a mobile phase that consisted of water (solvent A) and acetonitrile (solvent B) delivered in gradient elution mode at a flow rate of 0.6 ml min^{-1}. The elution program was as follows: 0 to 0.5 min, 5% solvent B; 0.5 to 3 min, 60% solvent B; 3 to 3.1 min, 60% solvent B; 3.1 to 3.2 min, 5% solvent B, 3.2 to 10 min, 5% solvent B. Mass scans were measured from *m/z* 10 up to *m/z* 500 at a 350°C interface temperature, a 250°C desolvation line (DL) temperature, and a ±4,500-V interface voltage with a neutral DL/Qarray, using N_2 as the nebulizing and drying gas. Mass spectrometry data were acquired both in the positive ionization mode and in the negative ionization mode. The data were analyzed using LabSolutions LCMS software.

For isolation of the intermediate metabolites, bacteria were removed from the bioconversion reaction mixtures by centrifugation at 4,000 × *g* for 20 min, and the supernatants were evaporated under reduced pressure. The product of *hpoBCDF* was extracted with ethanol. Flash chromatography was performed on Kieselgel Si60 columns (40 to 63 μm; Merck) equilibrated with $CHCl_3$ and eluted with a $CHCl_3$-methanol gradient. The isolated intermediate metabolites were used for structural analysis and for the whole-cell and enzyme experiments.

The structures of the bioconversion products were determined using ^1H nuclear magnetic resonance (NMR) and ^{13}C NMR. ^1H and ^{13}C NMR spectra were recorded on a Varian Unity Inova 300 spectrometer (300 and 75 MHz, respectively). All products were dissolved in deuterated dimethyl sulfoxide (DMSO). Spectra were calibrated with respect to the solvent signal (for $CDCl_3$, ^1H δ = 7.26 and ^{13}C δ = 77.2; for DMSO-d_6, ^1H δ = 2.50 and ^{13}C δ = 39.5).

HpoI expression and purification. The *hpoI* gene was cloned into the expression vector pET28b(+) to obtain a protein tagged with 6His at the N terminus (Table 1). *E. coli* BL21(DE3) cells were transformed with the recombinant plasmid pET28-hpoI and cultivated as mentioned above. Cells were collected by centrifugation, washed with 50 mM potassium phosphate buffer (pH 7.2), resuspended in 8 ml of the same buffer, and disrupted by sonication. Cell debris was removed by centrifugation at 16,000 × *g* for 10 min. Cell extracts were loaded onto a HiTrap IMAC FF 5-ml nickel column (GE Healthcare), and proteins were eluted with 50 mM potassium phosphate buffer, pH 7.2, containing 0.5 M imidazole. The purity of HpoI was confirmed by electrophoresis on a 14% SDS-polyacrylamide gel.

Chemical synthesis of 2-ketoglutaramate. 2-Ketoglutaramate was prepared according to a previously published procedure (21). Fremy's salt (0.75 mM) was added to a 0.25 mM solution of glutamine prepared in sodium bicarbonate buffer (1 M, pH 9.5). The reaction mixture was stirred at room temperature and monitored daily by thin-layer chromatography. The glutamine was completely converted to 2-ketoglutaramate in 5 days. The reaction mixture was neutralized (final pH, 6.0) by addition of Dowex-50WX8-100 ion-exchange resin and then filtered and analyzed by HPLC-MS.

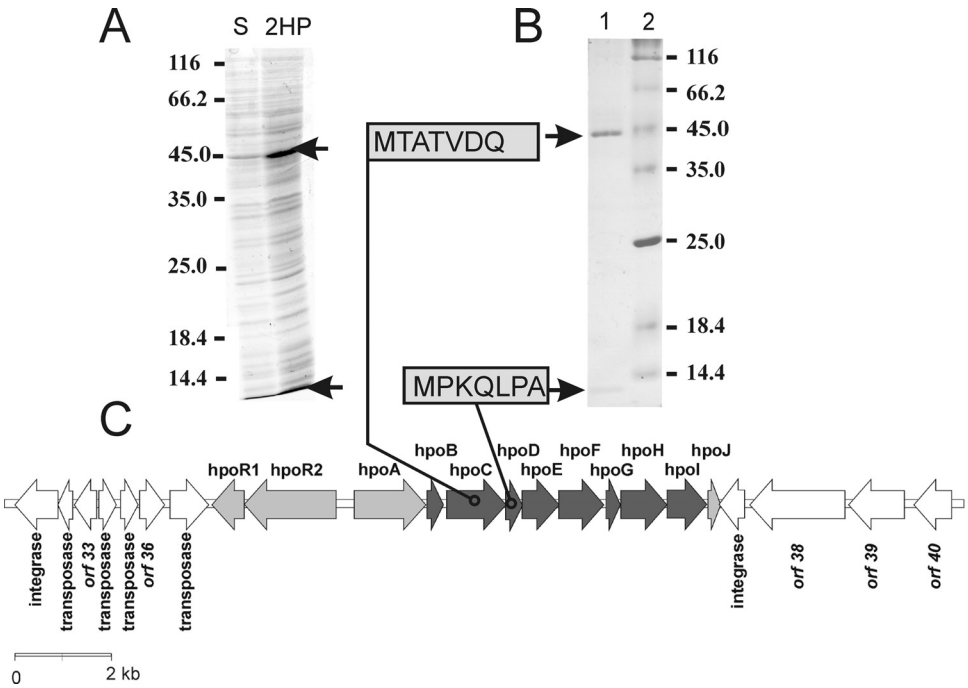

FIG 2 2HP-inducible proteins. (A) *Rhodococcus rhodochrous* PY11 was cultivated in minimal medium supplemented with 0.1% succinate (lane S) or 0.1% 2HP as a single source of carbon (lane 2HP). The positions of molecular mass markers are shown (in kilodaltons) to the left of the gels. (B) Purification of 2HP-inducible proteins (lane 1) and determination of N-terminal sequences. SDS-polyacrylamide gels were stained with Coomassie blue. Arrows, 2HP-inducible proteins. The positions of molecular mass markers (lane 2) are shown (in kilodaltons) to the right of the gels. (C) Genetic organization of the *hpo* gene locus, which is involved in the metabolism of 2HP in *Rhodococcus rhodochrous* PY11, and its flanking regions. Black arrows, genes that are known to be involved in 2HP degradation; gray arrows, transport system and regulatory gene; white arrows, other open reading frames (ORFs) in the locus.

ω-Amidase assay. Purified recombinant HpoI (100 μg) was added to reaction mixtures (of 250 μl) containing different concentrations of 2-ketoglutaramate in 50 mM potassium phosphate, pH 7.2. Samples were incubated at 30°C for 16 h, and the reactions were stopped by adding equal amount of acetonitrile. The formation of α-ketoglutarate was monitored by HPLC-MS.

Gene sequence analysis. The similarity of the deduced amino acid sequences of the proteins encoded by the *hpo* locus with sequences in the NCBI database was performed using the BLAST program (22). Protein functions were assigned on the basis of the similarity of the protein amino acid sequences with the sequences in the NCBI Conserved Domain Database (CDD) (23).

Nucleotide sequence accession numbers. The *Rhodococcus rhodochrous* PY11 genome fragment sequence with the 2HP degradation locus was deposited in GenBank under accession no. FM202432. The *Rhodococcus rhodochrous* PY11 16S rRNA gene sequence was deposited in GenBank under accession no. KT951673. The *Rhodococcus rhodochrous* PY11 strain was deposited in the DSMZ open collection as strain DSM 101666.

RESULTS AND DISCUSSION

Identification of genes involved in degradation of 2HP. We reported previously that *Rhodococcus rhodochrous* PY11 is capable of using 2HP as a source of carbon and energy (14). The 16S rRNA gene sequence of strain PY11 showed 99% similarity to that of bacteria of the *Rhodococcus rhodochrous* group and 96.0 to 98% similarities to the 16S rRNA gene sequences of other type strains of the genus *Rhodococcus* (see Fig. S1 in the supplemental material). On the basis of the results of 16S rRNA gene sequence analysis and biochemical tests (see the supplemental material), strain PY11 was identified to be *Rhodococcus rhodochrous* PY11. Two approaches were followed to identify the genes encoding the degradation of 2HP: (i) the technique of mRNA differential display to identify 2HP-inducible genes in *Rhodococcus rhodochrous* PY11 and (ii) analysis of 2HP-inducible proteins.

In total, 19 DNA fragments generated from the RNA of induced cells but not from the RNA of control cells were sequenced, and the sequences were compared with those in GenBank. The 350-bp fragment (2HP3) encoded a 98-amino-acid protein that showed homology (72% identity; E value, 2.1E−27) to the hypothetical protein gpORF106 from *Arthrobacter nicotinovorans* (10) (see Fig. S2 in the supplemental material). Although the function of gpORF106 has not been determined yet, the *orf106* gene was found to be located in a cluster responsible for nicotine biodegradation in *Arthrobacter nicotinovorans* (10). Therefore, the aforementioned 350-bp DNA fragment, containing a full gene (later designated *hpoG*), was used as a probe for chromosome walking to identify a genomic locus putatively encoding 2HP biodegradation in *Rhodococcus rhodochrous* PY11. Hence, a 60,152-bp-long DNA fragment from the genome of *Rhodococcus rhodochrous* PY11 (GenBank accession no. FM202432) was cloned into several plasmids for sequencing.

SDS-PAGE analysis revealed that at least one 2HP-inducible protein was detectable in *Rhodococcus rhodochrous* PY11 (Fig. 2A). During the purification of this protein (45 kDa), another product of 14 kDa was also copurified (Fig. 2B). Both the 45-kDa and 14-kDa proteins were subjected to N-terminal amino acid sequencing, which allowed us to map their corresponding genes (designated *hpoC* and *hpoD*, respectively) within the sequenced 60-kb genome fragment. By combining the data obtained from the mRNA differential display with those from the analysis of

TABLE 2 Functional annotations of hypothetical Hpo proteins

Protein	Size (amino acids)	Putative function	Superfamily designation			
			Region (positions)	Superfamily (specific hit/conserved domain)	CDD accession no.	E value
HpoR1	222	DNA binding response regulator	17–131	REC (signal receiver domain)	cd00156	1.92E−22
			161–217	LuxR_C_like	cd06170	5.87E−17
HpoR2	632	Signal transduction histidine kinase	18–242	PAS domain	cd00130	2.26E−06
			263–324	HisKA (histidine kinase A)	cd00082	1.86E−15
			398–483	HATPase_c (histidine kinase-like ATPases)	cd00075	3.18E−20
			515–629	REC (signal receiver domain)	cd00156	7.62E−24
HpoA	494	Permease	8–357	SLC5-6_like_sbd (nucleobase-cation symport 1 transporters)	cd10323	2.04E−06
HpoB	114	Ferredoxin	3–101	Rieske (Rieske_RO_ferredoxin)	cd03528	8.77E−38
HpoC	409	Large subunit of aromatic ring-hydroxylating dioxygenase	57–183	Rieske (Rieske_RO_alpha_N)	cd03469	5.03E−33
			208–404	SRPBCC (RHO_alpha_C)	cd00680	9.14E−36
HpoD	116	Small subunit of aromatic ring-hydroxylating dioxygenase		No putative conserved domains have been detected		
HpoE	253	Short-chain dehydrogenase/reductase	7–248	NADB Rossmann (SDR_C)	cd05233	1.29E−61
HpoF	310	Ferredoxin-NADPH reductase	9–213	FNR_like (ferredoxin reductase/PDR_like phthalate dioxygenase reductase)	cd06185	2.75E−86
			226–304	Fer2 (2Fe-2S iron-sulfur cluster binding domain)	cd00207	3.17E−11
HpoG	98	Hypothetical protein	2–95	Dabb (stress-responsive A/B barrel domain)	pfam07876	3.04E−19
HpoH	320	Cyclase	52–252	Cyclase	pfam04199	1.76E−37
HpoI	275	Nitrilase	7–269	Nitrilase	cd07583	3.2E−108

2HP-inducible proteins and bioinformatics sequence analysis, the operon putatively involved in the biodegradation of 2HP in *Rhodococcus rhodochrous* PY11 was identified. The operon consisted of 12 genes, denominated *hpoR1*, *hpoR2*, *hpoA*, *hpoB*, *hpoC*, *hpoD*, *hpoE*, *hpoF*, *hpoG*, *hpoH*, *hpoI*, and *hpoJ* (Table 2; Fig. 2C).

The *hpo* gene cluster is surrounded by transposases, integrases, and a truncated *hpoJ* gene (Fig. 2C), suggesting a horizontal gene transfer event. The first two genes in the *hpo* operon, designated *hpoR1* and *hpoR2*, encode a potential two-component regulatory system (Table 2; see also Tables S1 and S2 in the supplemental material). The amino acid sequence of HpoA showed similarity to bacterial permeases for cytosine/purines, uracil, thiamine, and allantoin. The homologs of HpoA participate in the transport of *N*-heterocyclic compounds. This allows us to assume that this protein is responsible for the intake of 2HP; however, further investigation is required to elucidate the precise function of this protein.

The *hpoBCDF* genes encode the 2HP four-component dioxygenase. A BLAST homology search against database sequences revealed that the genes *hpoB*, *hpoC*, and *hpoF* share amino acid sequence similarity with the ferredoxin, large subunit, and ferredoxin reductase components of the ring-hydroxylating dioxygenases, respectively (Table 2). The bioinformatics analysis showed that HpoD has no putative conserved domains; however, results from protein analysis experiments (Fig. 2B) revealed that this protein forms a strong complex with HpoC. Thus, we hypothesized that HpoD may function as a small subunit of the dioxygenase system.

To investigate the role of the initial oxidation of 2HP, the *hpoB*, *hpoC*, *hpoD*, and *hpoF* genes were cloned and expressed in *E. coli*. pET-28b, pETDuet-1, and pCDFDuet-1 (Table 1) were used to construct a set of compatible plasmids, each carrying either an individual gene from the *hpo* cluster or a different combination of three *hpo* genes. Then, the ability of *E. coli* BL21(DE3) cells transformed with the *hpo* locus genes to metabolize 2HP was analyzed. As seen in Fig. S3 in the supplemental material, the cells carrying the *hpoBCDF* genes were able to completely transform 2HP within 1 h. By expressing different combinations of three *hpo* genes, we identified that only three Hpo proteins, namely, HpoB (a putative ferredoxin), HpoC (a putative large subunit of dioxygenase), and HpoD (a putative small subunit of dioxygenase), are essential for the initial attack of the pyridine ring of 2HP (Fig. 3). The *hpoF* gene could be replaced by other intrinsic *E. coli* ferredoxin reductases, a finding consistent with the findings of many other studies of dioxygenases (24). Our data suggest that HpoBCDF proteins form the dioxygenase system that catalyzes the oxidation of 2HP.

According to the literature, several dioxygenases show promiscuous activity toward pyridine derivatives; e.g., a naphthalene dioxygenase from *Pseudomonas* sp. strain NCIB 9816-4 oxidizes *N*-methyl-2-pyridone derivatives but not 2-pyridone (25), while a mutant toluene dioxygenase from *Pseudomonas putida* F1 is active toward 4-picoline (26). On the contrary, HpoBCDF from *Rhodococcus rhodochrous* PY11 uses 2HP as a physiological substrate.

Identification of 2HP oxidation product. To identify the reaction product of the oxidation of 2HP by the HpoBCDF dioxygenase system, *E. coli* BL21(DE3) cells carrying pB/D and pF/C (harboring the *hpoBCDF* genes) were used to transform larger amounts of 2HP. After a flash column purification of the product, HPLC-MS, ^{13}C NMR, and ^{1}H NMR analyses were performed (see the text in the supplemental material). The product of 2HP oxidation was identified to be 3,6-dihydroxy-1,2,3,6-tetrahydropyridin-2-one. This compound was rather unstable and under acidic conditions was rapidly transformed to 2,5DHP (data not shown). According to the literature, the *cis*-dihydrodiols of *N*-heterocycles are relatively unstable; e.g., higher temperatures (~50°C) lead to their *trans* isomerization, while mild acid conditions cause dehy-

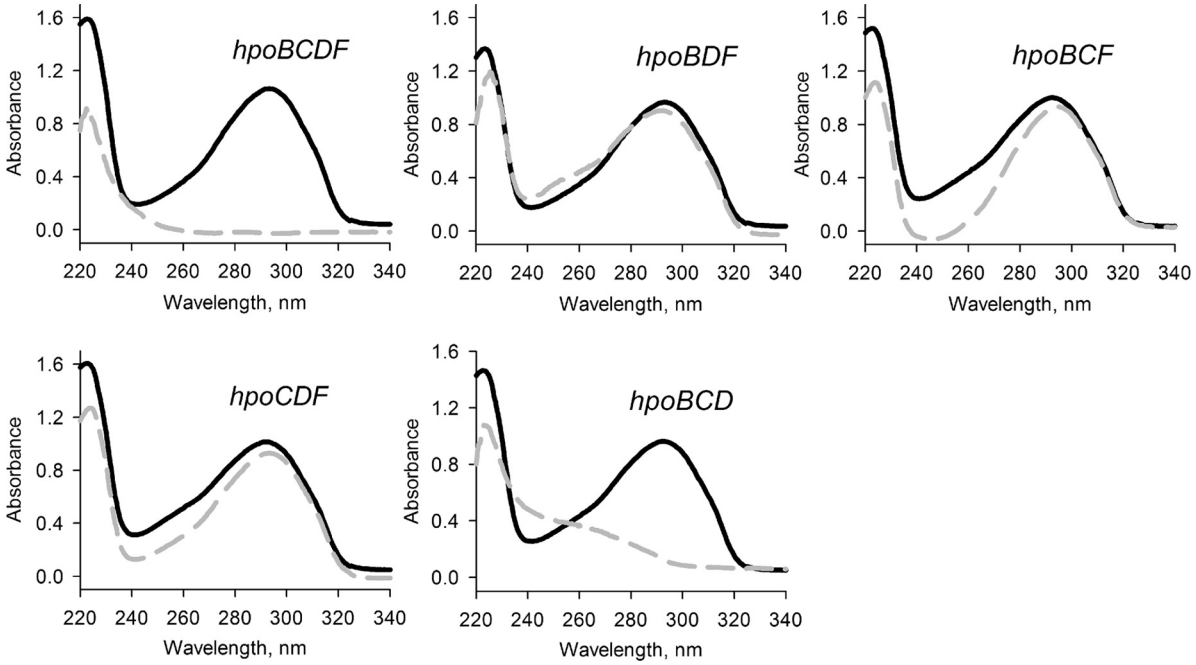

FIG 3 Bioconversion of 2HP in *E. coli* transformed with compatible plasmids, each carrying a different combination of genes from the *hpo* locus. Cultures of *E. coli* were incubated in potassium phosphate buffer supplemented with 0.2 mM 2HP for 5 h, and the UV absorption spectra were recorded. Black solid lines, initial spectrum of 2HP; gray dashed lines, the final spectra of the bioconversion products.

dration (27). The expected product of the aromatic ring-hydroxylating dioxygenase is *cis*-diol. We hypothesize that the true product of HpoBCDF dioxygenase is in fact a *cis*-5,6-dihydro-5,6-dihydroxy-2-pyridone, which is undetectable outside the cell due to its instability.

The substrate specificity of the dioxygenase system was tested with various pyridinols as the substrates. Out of 15 *N*-heterocyclic aromatic compounds tested (see Table S3 in the supplemental material), only 2-hydroxy-3-methylpyridine was transformed by *E. coli* BL21(DE3) cells carrying pB/D and pF/C (carrying the *hpoBCDF* genes). The product of 2-hydroxy-3-methylpyridine oxidation was purified and identified to be 3,6-dihydroxy-5-methyl-1,2,3,6-tetrahydropyridin-2-one (see the text in the supplemental material).

HpoE catalyzes the second step in 2HP biodegradation. The sequence of the deduced *hpoE* gene product showed a significant similarity to the sequences of short-chain dehydrogenases/reductases. Several proteins of this family are encoded by bacterial operons responsible for the biodegradation of aromatic compounds, and these operons are usually located in close proximity to the genes that encode dioxygenases. Such dehydrogenases catalyze the oxidation of *cis*-dihydrodiols, the products of the dioxygenase enzymatic reaction, to form the corresponding catechols (28). Since all our attempts to express *hpoE* in *E. coli* were unsuccessful due to the production of insoluble protein aggregates, *R. erythropolis* strain SQ1, incapable of transforming 2HP, was used for the expression of HpoE. For this, the *hpoE* gene was cloned into pART2 (Table 1), and the recombinant plasmid pART2HpoE was used to transform *R. erythropolis* SQ1 cells. Although in the case of the latter strain the recombinant protein was soluble, no activity of HpoE could be detected *in vitro* or *in vivo* using 3,6-dihydroxy-1,2,3,6-tetrahydropyridin-2-one as a substrate.

To confirm that HpoE is indeed responsible for the catalysis of the second step in the biodegradation of 2HP, the DNA fragment harboring the *hpoB*, *hpoC*, *hpoD*, *hpoE*, *hpoF*, and *hpoG* genes was cloned into the pHpoBCDEFG plasmid. After transformation of *R. erythropolis* SQ1 cells with pHpoBCDEFG, the bacteria produced the blue pigment in the presence of 2HP (Fig. 4B; see also Fig. S4 in the supplemental material). A pigment with similar physical characteristics (UV-visible spectra and molecular mass) was shown to be produced by *Arthrobacter oxydans* grown on nicotine (9), and the nicotine blue is formed via the autoxidation of THP. We cloned a DNA fragment with the *hpoB*, *hpoC*, and *hpoD* genes into the pNitQC1 plasmid to obtain pNitHpoBCD. After transformation of *R. erythropolis* SQ1 cells with pNitHpoBCD, the bacteria could convert 2HP to 3,6-dihydroxy-1,2,3,6-tetrahydropyridin-2-one, as was the case with *E. coli* BL21(DE3) cells carrying the *hpoBCD* genes. In the presence of 2HP, *R. erythropolis* SQ1 cells harboring the pNitHpoBCD and pART2HpoE plasmids could produce the blue pigment far less efficiently than those carrying pHpoBCDEFG. This may be due to the different protein expression levels or the absence of HpoF and HpoG. Therefore, the *hpoE* gene was assigned to be a putative 2-pyridone-5,6-dihydro-*cis*-5,6-diol dehydrogenase that catalyzes the second step in 2HP degradation (Fig. 5). Though HpoG is phylogenetically related to stress response proteins and those of unknown function, its closest homolog is *orf106* (*mox*) from *Arthrobacter nicotinovorans*. *orf106* (*mox*) is located within a gene cluster that is involved in degradation of the plant alkaloid nicotine (10), yet the exact function of this gene has never been elucidated. *hpoG* expression was induced in *Rhodococcus rhodochrous* PY11 in the presence of 2HP, but the function of the HpoG protein remains unknown.

HpoH is a hydrolase active toward THP. The next step of the

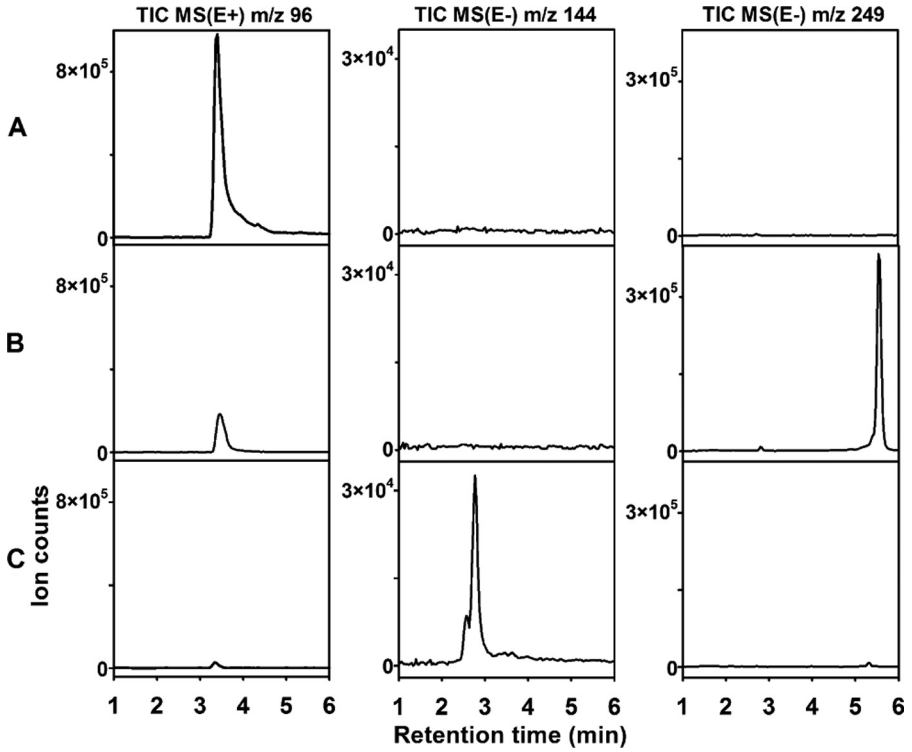

FIG 4 Conversion of 2HP in *Rhodococcus erythropolis* SQ1 transformed with recombinant plasmids, each carrying a different combination of genes from the *hpo* locus. (A) *R. erythropolis* SQ1 (control without plasmids); (B) *R. erythropolis* SQ1 harboring the pHpoBCDEFG plasmid; (C) *R. erythropolis* SQ1 transformed with pHpoBCDEFG and pNitHpoH. For HPLC-MS analysis, cultures of *Rhodococcus erythropolis* SQ1 were incubated in potassium phosphate buffer supplemented with 0.2 mM 2HP for 2 h. The total-ion chromatograms (TIC) were recorded in the positive-ion (E+) or negative-ion (E−) mode from the MS.

2HP degradation pathway is ring fission. Although *N*-heterocycles are usually oxidatively cleaved by dioxygenases (1, 3), the hydrolytic cleavage of the pyridine ring was proposed in *Rhodococcus opacus* (13), *A. nicotinovorans*, *Nocardioides* sp. strain JS614, and *R. opacus* (12), yet to our knowledge, no protein/gene has been shown to be responsible for THP (the precursor of the blue pigment) metabolism to date, probably due to the high degree of instability of THP. In the case of *Rhodococcus rhodochrous* PY11, the primary structure of the *hpoH* gene product is similar to that of members of the cyclase superfamily. A BLAST search against the sequences in the Protein Data Bank (PDB) revealed that the sequence of the HpoH protein shows similarity to the sequences of a predicted metal-dependent hydrolase from *Bacillus stearothermophilus* (PDB accession no. 1R61) and a manganese-dependent isatin hydrolase from *Labrenzia aggregata* IAM 12614 (PDB accession no. 4J0N) (29) (with 26% and 23% sequence identity, respectively), both of which belong to the cyclase superfamily. Three-dimensional structure analysis of these two proteins revealed that the conserved cyclase motif **H**XGT**H**X**D**XPXH is responsible for the complexation of metal ions (two histidines and a glutamate are

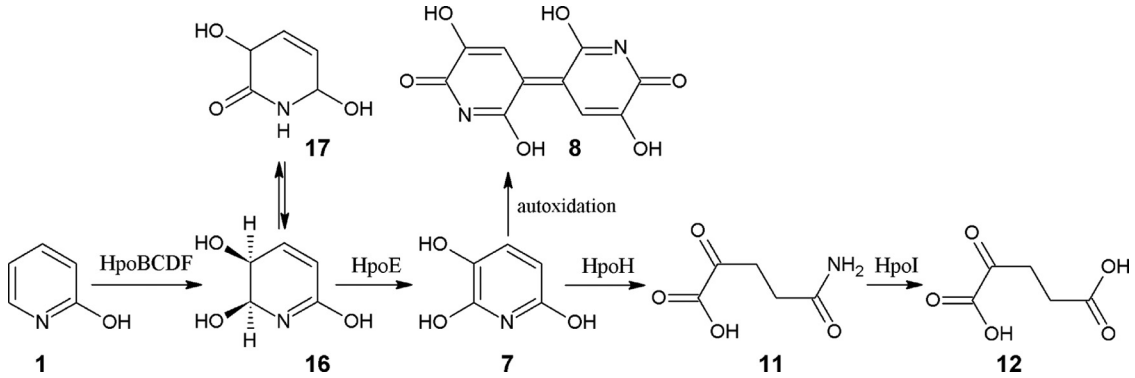

FIG 5 Proposed 2-hydroxypyridine catabolic pathway in *Rhodococcus rhodochrous* PY11. Compound 1, 2-hydroxypyridine; compound 16, *cis*-5,6-dihydro-5,6-dihydroxy-2-pyridone; compound 17, 3,6-dihydroxy-1,2,3,6-tetrahydropyridin-2-one; compound 7, 2,3,6-trixydroxypyridine; compound 8, nicotine blue pigment; compound 11, 2-ketoglutaramate; compound 12, α-ketoglutarate. HpoBCDF, four-component dioxygenase; HpoE, 2-pyridone-5,6-dihydro-*cis*-5,6-diol dehydrogenase; HpoH, THP hydrolase; HpoI, 2-ketoglutaramate amidase.

shown in bold). Therefore, it is natural to assume that cyclase could function as a hydrolase in the presence of appropriate metal ions. Moreover, in all known bacteria that produce a blue pigment from nicotine, the homologs of *hpoH* are located in close proximity to operons confirmed to be responsible for nicotine degradation (12). Thus, we hypothesized that *hpoH* may encode the hydrolytic ring-opening activity.

To test this hypothesis, the *hpoH* gene was cloned into the pNitQC1 plasmid to obtain pNitHpoH. After cotransformation of *R. erythropolis* SQ1 with the pHpoBCDEFG and pNitHpoH plasmids, the bacteria did not produce a blue pigment in the presence of 2HP but still retained the ability to metabolize this compound. HPLC-MS analysis of the reaction products revealed a new compound with a molecular mass of 145 Da (Fig. 4C), which corresponded well to the molecular mass of hydrolyzed THP, confirming our hypothesis that the latter compound undergoes hydrolytic cleavage.

In water, THP exists in several tautomeric forms, one of which is 3-hydroxypyridine-2,6(1*H*,3*H*)-dione. The most likely bond to be hydrolyzed in THP is one of the amide bonds. If such is the case, two products of THP hydrolysis by HpoH are possible: either 2-ketoglutaramate or 4-ketoglutaramate. The HPLC retention time of a chemically synthesized 2-ketoglutaramate was identical to that of the product of THP hydrolysis by HpoH (see Fig. S5 in the supplemental material). Thus, the results presented here indicate that the hypothetical cyclase HpoH is in fact a THP hydrolase.

The *hpoI* gene encodes a ω-amidase for 2-ketoglutaramate. It was recently shown that three Gram-positive soil bacteria, namely, *Arthrobacter nicotinovorans*, *Nocardioides* sp. JS614, and *Rhodococcus opacus*, all contain a homologous nitrilase gene located within the gene cluster responsible for nicotine catabolism (12). Moreover, it was confirmed experimentally that the aforementioned nitrilase catalyzed the conversion of 2-ketoglutaramate to α-ketoglutarate (12). The amino acid sequence of HpoI from *Rhodococcus rhodochrous* PY11 showed significant similarity to these nitrilases and contained the conserved Cys-Glu-Lys triad involved in catalysis (12). We suggested above that the THP hydrolase may generate 2-ketoglutaramate as a final product. The recombinant HpoI protein expressed in *E. coli* exhibited ω-amidase activity with 2-ketoglutaramate as a substrate (see Fig. S5 in the supplemental material). When a product of THP hydrolysis was incubated with a recombinant HpoI protein, the molecular mass of the generated compound increased by 1 Da, and its HPLC retention time matched that of α-ketoglutarate. These results strongly indicate that the final products of 2HP degradation in *Rhodococcus rhodochrous* PY11 are ammonium ion and α-ketoglutarate, which is a key intermediate in the Krebs cycle.

Conclusions. A 60-kb genomic fragment containing genes that are responsible for the degradation of 2HP in *Rhodococcus rhodochrous* PY11 was identified and investigated. The first reaction of 2HP degradation is catalyzed by the four-component HpoBCDF dioxygenase. The second enzymatic step in 2HP degradation is oxidation of *cis*-5,6-dihydro-5,6-dihydroxy-2-pyridone to render THP. This reaction is catalyzed by the *hpoE* gene product, whose primary structure is similar to the primary structures of short-chain dehydrogenases/reductases. After the initial hydroxylation, the next step in the aerobic degradation of cyclic aromatic compounds is a ring cleavage. We experimentally confirmed that the *hpoH* gene product catalyzes the hydrolytic ring opening of THP and identified the missing link in THP degradation. The product of THP hydrolysis is further metabolized via a hydrolysis reaction catalyzed by HpoI. The recombinant HpoI nitrilase converted 2-ketoglutaramate to α-ketoglutarate.

A complete set of genes responsible for aerobic 2HP degradation in *Rhodococcus rhodochrous* PY11 was identified and successfully expressed in heterologous hosts. The isolation of intermediate metabolites and their subsequent analysis allowed us to fully elucidate the catabolic pathway of 2HP. Our results enrich the understanding of the degradation pathways of *N*-heterocyclic aromatic compounds and provide further insights into the chemistry and biochemistry of the bacterial degradation of xenobiotics.

ACKNOWLEDGMENTS

We thank C. Sandu and T. Tamura for the pART and pNIT vectors. We thank Laura Kaliniene for helping to prepare the manuscript.

This work was supported by the European Social Fund (ESF) under the Human Resources Development Action Programme, the Global Grant measure, project no. VP1-3.1-ŠMM-07-K-03-015, from the Research Council of Lithuania.

We declare no conflict of interest.

FUNDING INFORMATION

Lietuvos Mokslo Taryba (Research Council of Lithuania) provided funding to Justas Vaitekūnas, Renata Gasparavičiūtė, Rasa Rutkienė, Daiva Tauraitė, and Rolandas Meškys under grant number VP1-3.1-ŠMM-07-K-03-015.

REFERENCES

1. **Kaiser JP, Feng Y, Bollag JM.** 1996. Microbial metabolism of pyridine, quinoline, acridine, and their derivatives under aerobic and anaerobic conditions. Microbiol Rev **60:**483–498.
2. **Shukla OP.** 1984. Microbial transformation of pyridine compounds. Proc Indian Acad Sci Chem Sci **93:**1143–1153.
3. **Fetzner S.** 1998. Bacterial degradation of pyridine, indole, quinoline, and their derivatives under different redox conditions. Appl Microbiol Biotechnol **49:**237–250. http://dx.doi.org/10.1007/s002530051164.
4. **Kolenbrander PE, Weinberger M.** 1977. 2-Hydroxypyridine metabolism and pigment formation in three *Arthrobacter* species. J Bacteriol **132:**51–59.
5. **Cain RB, Houghton C, Wright KA.** 1974. Microbial metabolism of the pyridine ring. Metabolism of 2- and 3-hydroxypyridines by the maleamate pathway in *Achromobacter* sp. Biochem J **140:**293–300.
6. **Shukla OP, Kaul SM.** 1986. Microbiological transformation of pyridine N-oxide and pyridine by *Nocardia* sp. Can J Microbiol **32:**330–341. http://dx.doi.org/10.1139/m86-065.
7. **Jiménez JI, Canales A, Jiménez-Barbero J, Ginalski K, Rychlewski L, García JL, Díaz E.** 2008. Deciphering the genetic determinants for aerobic nicotinic acid degradation: the nic cluster from *Pseudomonas putida* KT2440. Proc Natl Acad Sci U S A **105:**11329–11334. http://dx.doi.org/10.1073/pnas.0802273105.
8. **Stanislauskiene R, Gasparaviciute R, Vaitekunas J, Meskiene R, Rutkiene R, Casaite V, Meskys R.** 2012. Construction of *Escherichia coli-Arthrobacter-Rhodococcus* shuttle vectors based on a cryptic plasmid from *Arthrobacter rhombi* and investigation of their application for functional screening. FEMS Microbiol Lett **327:**78–86. http://dx.doi.org/10.1111/j.1574-6968.2011.02462.x.
9. **Knackmuss HJ, Beckmann W.** 1973. The structure of nicotine blue from *Arthrobacter oxidans*. Arch Mikrobiol **90:**167–169. http://dx.doi.org/10.1007/BF00414521.
10. **Baitsch D, Sandu C, Brandsch R, Igloi GL.** 2001. Gene cluster on pAO1 of *Arthrobacter nicotinovorans* involved in degradation of the plant alkaloid nicotine: cloning, purification, and characterization of 2,6-dihydroxypyridine 3-hydroxylase. J Bacteriol **183:**5262–5267. http://dx.doi.org/10.1128/JB.183.18.5262-5267.2001.
11. **Gupta RC, Shukla OP.** 1975. Microbial metabolism of 2-hydroxypyridine. Indian J Biochem Biophys **12:**296–298.
12. **Cobzaru C, Ganas P, Mihasan M, Schleberger P, Brandsch R.** 2011. Homologous gene clusters of nicotine catabolism, including a new omega-amidase for alpha-ketoglutaramate, in species of three genera of Gram-

positive bacteria. Res Microbiol **162:**285–291. http://dx.doi.org/10.1016/j.resmic.2011.01.001.

13. **Zefirov NS, Agapova SR, Terentiev PB, Bulakhova IM, Vasyukova NI, Modyanova LV.** 1994. Degradation of pyridine by *Arthrobacter crystallopoietes* and *Rhodococcus opacus* strains. FEMS Microbiol Lett **118:**71–74. http://dx.doi.org/10.1111/j.1574-6968.1994.tb06805.x.
14. **Semėnaitė R, Gasparavičiūtė R, Duran R, Precigou S, Marcinkevičienė L, Bachmatova I, Meškys R.** 2003. Genetic diversity of 2-hydroxypyridine-degrading soil bacteria. Biologija **2:**27–29.
15. **Quan S, Dabbs ER.** 1993. Nocardioform arsenic resistance plasmid characterization and improved *Rhodococcus* cloning vectors. Plasmid **29:**74–79. http://dx.doi.org/10.1006/plas.1993.1010.
16. **Sandu C, Chiribau C-B, Sachelaru P, Brandsch R.** 2005. Plasmids for nicotine-dependent and -independent gene expression in *Arthrobacter nicotinovorans* and other *Arthrobacter* species. Appl Environ Microbiol **71:**8920–8924. http://dx.doi.org/10.1128/AEM.71.12.8920-8924.2005.
17. **Nakashima N, Tamura T.** 2004. Isolation and characterization of a rolling-circle-type plasmid from *Rhodococcus erythropolis* and application of the plasmid to multiple-recombinant-protein expression. Appl Environ Microbiol **70:**5557–5568. http://dx.doi.org/10.1128/AEM.70.9.5557-5568.2004.
18. **Sambrook J, Russell DW.** 2001. Molecular cloning: a laboratory manual, 3rd ed. Cold Spring Harbor Laboratory Press, Cold Spring Harbor, NY.
19. **Sharkey FH, Banat IM, Marchant R.** 2004. A rapid and effective method of extracting fully intact RNA from thermophilic geobacilli that is suitable for gene expression analysis. Extremophiles **8:**73–77. http://dx.doi.org/10.1007/s00792-003-0363-2.
20. **Brzostowicz PC, Gibson KL, Thomas SM, Blasko MS, Rouvière PE.** 2000. Simultaneous identification of two cyclohexanone oxidation genes from an environmental *Brevibacterium* isolate using mRNA differential display. J Bacteriol **182:**4241–4248. http://dx.doi.org/10.1128/JB.182.15.4241-4248.2000.
21. **Martinez RA, Unkefer PJ.** September 2001. Preparation of 2-hydroxy-5-oxoproline and analogs thereof. US patent 6,288,240 B1.
22. **Pearson WR, Lipman DJ.** 1988. Improved tools for biological sequence comparison. Proc Natl Acad Sci U S A **85:**2444–2448. http://dx.doi.org/10.1073/pnas.85.8.2444.
23. **Marchler-Bauer A, Lu S, Anderson JB, Chitsaz F, Derbyshire MK, DeWeese-Scott C, Fong JH, Geer LY, Geer RC, Gonzales NR, Gwadz M, Hurwitz DI, Jackson JD, Ke Z, Lanczycki CJ, Lu F, Marchler GH, Mullokandov M, Omelchenko MV, Robertson CL, Song JS, Thanki N, Yamashita RA, Zhang D, Zhang N, Zheng C, Bryant SH.** 2011. CDD: a Conserved Domain Database for the functional annotation of proteins. Nucleic Acids Res **39:**D225–D229. http://dx.doi.org/10.1093/nar/gkq1189.
24. **Gibson DT, Parales RE.** 2000. Aromatic hydrocarbon dioxygenases in environmental biotechnology. Curr Opin Biotechnol **11:**236–243. http://dx.doi.org/10.1016/S0958-1669(00)00090-2.
25. **Chopard C, Azerad R, Prangé T.** 2008. Naphthalene-dioxygenase-catalysed cis-dihydroxylation of azaarene derivatives. J Mol Catal B Enzym **50:**53–60. http://dx.doi.org/10.1016/j.molcatb.2007.09.013.
26. **Sakamoto T, Joern JM, Arisawa A, Arnold FH.** 2001. Laboratory evolution of toluene dioxygenase to accept 4-picoline as a substrate. Appl Environ Microbiol **67:**3882–3887. http://dx.doi.org/10.1128/AEM.67.9.3882-3887.2001.
27. **Modyanova L, Azerad R.** 2000. Dioxygenase-catalysed formation of dihydrodiol metabolites of N-methyl-2-pyridone. Tetrahedron Lett **41:**3865–3869. http://dx.doi.org/10.1016/S0040-4039(00)00541-4.
28. **Fong KP, Tan H-M.** 1999. Characterization of a novel *cis*-benzene dihydrodiol dehydrogenase from Pseudomonas putida ML2. FEBS Lett **451:**5–9. http://dx.doi.org/10.1016/S0014-5793(99)00520-7.
29. **Bjerregaard-Andersen K, Sommer T, Jensen JK, Jochimsen B, Etzerodt M, Morth JP.** 2014. A proton wire and water channel revealed in the crystal structure of isatin hydrolase. J Biol Chem **289:**21351–21359. http://dx.doi.org/10.1074/jbc.M114.568824.